

Growth and characterization of FeTe thin films under tensile strain

Hyunjee Song, Younsik Kim, Sangjae Lee, Suyoung Lee, Youngdo Kim, Yeonjae Lee, and Changyoung Kim*

Department of Physics and Astronomy, Seoul National University, Seoul 08826, Korea

(Received 6 December 2024; revised or reviewed 23 December 2024; accepted 24 December 2024)

Abstract

Iron chalcogenides exhibit a variety of emerging properties via substituting the chalcogenide atoms between Te, Se and S. The interplay between temperature, pressure, and composition in iron chalcogenides drives transitions between various phases, e.g., superconducting, magnetic, and structural phases. These phase behaviors are known to result from tuning the bond angle between Fe and chalcogenide atoms in such Fe-Ch compounds. By growing FeTe thin films on substrates via molecular beam epitaxy (MBE), we tune the epitaxial strain imposed on FeTe, and thus manipulate the Fe-Te bond angle. Our transport and angle-resolved photoemission spectroscopy (ARPES) measurements show that such modulation in the FeTe structure effectively modifies the underlying electronic structure, giving rise to various emerging properties different from those of bulk FeTe. We further propose to systematically investigate FeTe thin films to reveal novel phases inaccessible in bulk iron chalcogenides and study the origin of such emergent behaviors.

Keywords: superconductor, FeTe, molecular beam epitaxy (MBE)

1. INTRODUCTION

In condensed matter physics research, iron chalcogenides have attracted immense attention owing to their rich and tunable physical properties. Despite their simple tetragonal crystal structure, iron chalcogenides possess diverse properties such as bicollinear anisotropy in FeTe [1], topological superconductivity in $\text{FeSe}_{0.45}\text{Te}_{0.55}$ [2] and BCS-BES crossover in $\text{Fe}(\text{Se},\text{S})$ [3]. The close relationship between magnetism and superconductivity, along with the tunable nature of these materials makes iron chalcogenides an essential tool to get a better grasp of the mechanism of unconventional superconductivity [4-8].

A key parameter tuning aforementioned properties in iron chalcogenides is the bond angle between iron and chalcogen atoms [9]. It is well established that overall electronic correlation is highly dependent on the bond angle [9, 10]. This suggests that by controlling the bond angle, we can modulate physical properties or even reveal unknown phases of the matter.

As a way of engineering the bond angle between iron and chalcogenide atoms, we used strain effect induced by the lattice mismatch with the substrate. Epitaxial strain on thin films can act as an external pressure on bulk where tensile strain enlarges the bond angle and vice versa for compressive strain [11]. Especially when fabricating thin films with strain effects, it is crucial to have atomically clean interface and high stoichiometry as it is possible to observe the emergent phenomena on high quality thin films.

In this paper, we demonstrate the optimal growth condition of high-quality FeTe thin film in molecular beam

epitaxy (MBE). We report a signature of superconducting behavior in FeTe thin films with tensile strain via electrical transport measurements.

2. METHODS

FeTe thin films were deposited on (001)-oriented SrTiO_3 (STO) substrates in ultrahigh vacuum (UHV) using an MBE system which is one of the prominent techniques to grow thin films and heterostructures. We note that calculated from the lattice constants of FeTe and STO, FeTe thin films are estimated to be under tensile strain of 2%. STO substrates were treated with deionized water, buffered oxide etchant and annealed at a temperature of 1200 °C before the growth. Prior to the deposition, the substrates were annealed at 500 °C for 10 minutes.

Growth process was monitored in real time with an in-situ reflection high energy electron diffraction (RHEED) system. RHEED patterns allow us to probe the surface morphology. Sharp intense diffraction patterns indicate an atomically smooth, single-crystalline surface while 3D diffraction patterns are an evidence of amorphous and rough surface.

After the growth, gold electrodes were deposited ex-situ with a Hall bar geometry on FeTe thin films with an electron beam evaporator system for electrical transport measurements. Using Quantum Design Physical Property Measurement System, resistivity and Hall effect were measured.

* Corresponding author: changyoung@snu.ac.kr

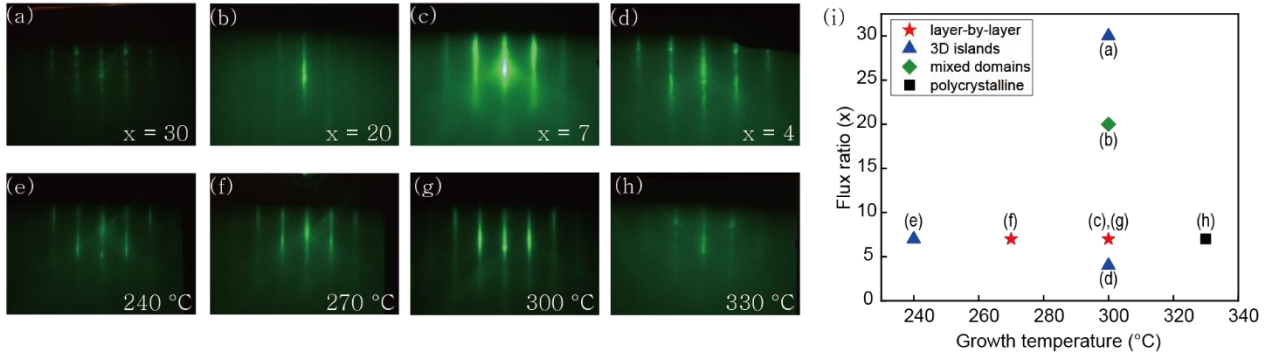


Fig. 1. RHEED images of (a) $x = 30$ (b) $x = 20$ (c) $x = 7$ (d) $x = 4$ with substrate temperature kept at 300 °C. Here, x is defined as the Te to Fe flux ratio. RHEED images of substrate temperature at (e) 240 °C (f) 270 °C (g) 300 °C (h) 330 °C with $x = 7$ fixed. (i) Plot of growth window of FeTe thin film.

3. RESULTS

Successful growth of defect-free and crystalline samples is a prerequisite to study the principal physical properties of the material. MBE technique is capable of precisely engineering various control parameters during the growth. When specific conditions are satisfied, the material can grow layer-by-layer along the crystallographic direction of the substrate. To establish the growth window of epitaxial FeTe thin film, we varied the 1) relative flux between Fe and Te and the 2) growth temperature.

In monitoring the growth mode of the film in real time, RHEED is the most commonly used tool. From the RHEED pattern images in Figure 1, we could optimize the growth condition. Figure 1(a)-(d) are RHEED images of thin films with evaporation of Te source 4 to 30 times more than Fe source. We hereafter define the flux ratio of Te to Fe as x . STO substrates were kept at 300 °C during growth. In Fig. 1(a) where $x = 30$, not only the intensity of RHEED pattern is evidently weak, but also there are indications of 3D islands above the streak. For $x = 20$, (see Fig. 1(b)) it has additional streaks between main streaks, which indicates that domains with different orientations are mixed. The brightest and clearest rods in the RHEED was observed in Fig. 1(c) when $x = 7$, which implies single crystalline surface. Lastly, for $x = 4$ in Fig. 1(d), 3D islands appear again.

As much as the flux rate between compositions plays an important role in the sample quality, the growth temperature greatly affects the growth mode of thin films. With flux ratio of Te to Fe fixed at 7:1, growth temperature of the STO substrate was varied between 240 °C and 330 °C as displayed in Figs. 1(e)-1(h). The sample in Fig. 1(e) deposited at 240 °C shows weak streaks along with 3D islands. On the other hand, the film grown at 330 °C (Fig. 1(h)) consists of rings over the pattern. With minor differences in intensities, samples grown at substrate temperatures of 270 °C to 300 °C (see Figs. 1(f) and 1(g)) demonstrated the most-streaky patterns.

Depending on these factors, samples can be categorized into four different modes which are layer-by-layer, 3D islands, mixed domains and polycrystalline.

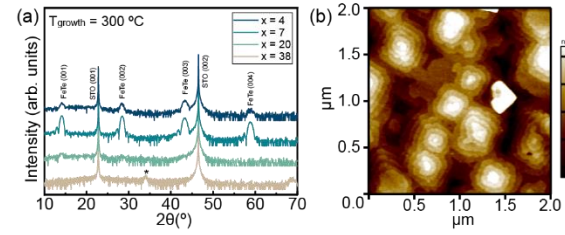


Fig. 1. (a) XRD measurements of samples in Figs. 1(a)-1(d).

*: peak of an impurity (b) AFM image of FeTe thin film.

They are plotted in Fig. 1(i). Hence, we were able to find the optimal growth condition for FeTe thin film: 7 times more Te flux than Fe, and growth temperature between 270 °C and 300 °C.

In order to reveal the crystalline structure, *ex-situ* X-ray diffraction was performed on samples grown with different flux ratios in Figs. 1(a)-1(d) and the results are plotted in Fig. 2(a). For the sample with a flux ratio of 30:1 (from Fig. 1(a)), there is no sign of FeTe and unknown impurity peak is observed. With a flux ratio of 20:1 (from Fig. 1(b)), impurity peaks are gone and a weak FeTe signal starts to appear. The sample in Fig. 1(c) with a flux ratio of 7:1 possesses the highest intensity for the FeTe peak without any sign of impurities. As the flux ratio decreases, FeTe peaks weaken again. Additionally, atomic force microscopy (AFM) measurements were performed on high quality samples in Fig. 1(c) and the results are shown in Fig. 2(b). The surface image displays rectangular shaped domains coming from its tetragonal crystal structure. Thus, from XRD and AFM results, we once again confirm that $x = 7$ and $T_{\text{growth}}=300^{\circ}\text{C}$ are the optimal growth condition of FeTe thin film on STO.

Small changes in the stoichiometry can greatly affect the emergent phenomena in the system [12-14]. To verify that synthesized FeTe thin films are stoichiometric, *in-situ* X-ray photoemission spectroscopy (XPS) measurements were carried out and the result is compared with that of single crystals [15] in Fig. 3. By analyzing the relative elemental composition and oxidation states of each element Fe 2p and Te 3d, we could confirm that our FeTe thin film has the same stoichiometry as a single crystal $\text{Fe}_{1.06}\text{Te}$.

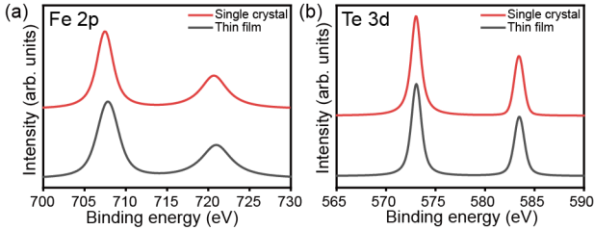


Fig. 3. XPS spectra of (a) Fe 2p and (b) Te 3d from thin film and single crystal FeTe.

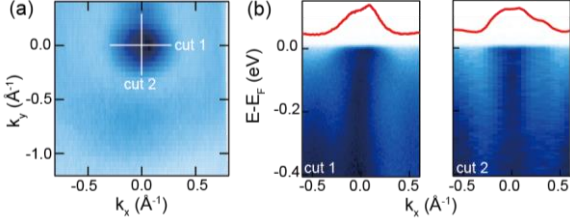


Fig. 4. Electronic structure of 5 u.c. FeTe/STO at 10 K (a) Fermi surface map at 10 K. (b) (left) cut 1 (right) cut 2.

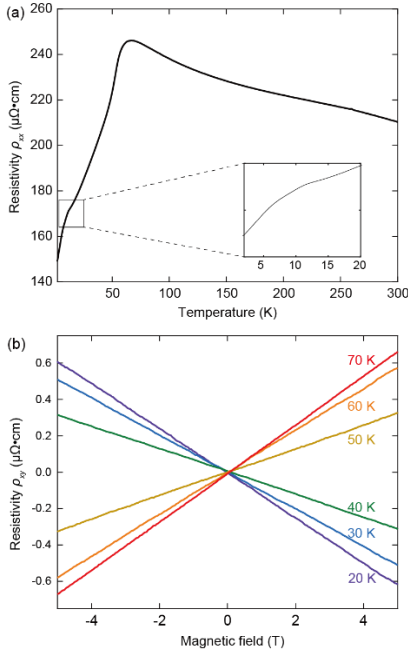


Fig. 5. (a) Resistivity and (b) Hall measurement results of 50 u.c. FeTe/STO.

Angle-resolved photoemission spectroscopy (ARPES) is a power tool to study the electronic structure of thin film systems. Since FeTe has a strong strain relaxation rate which is within few layers [16], observing the change in physical properties due to the strain effect is challenging. However, owing to surface-sensitivity of ARPES, it can probe the electronic states of the interface of thin films. With such advantage of ARPES technique, we measured the electronic structure of 5-unit cell FeTe thin film under influence of tensile strain as shown in Fig. 4. An electron pocket at the Γ point was well resolved as displayed in Fig. 4(b). One of the distinguishable differences between thin film and bulk is that for the thin film, a strong quasiparticle peak at Γ

point is not as apparent as it is in bulk [15]. Further systematic ARPES studies on thin films as a function of epitaxial strain are to be followed.

Finally, we performed *ex-situ* transport measurements of 50 u.c. FeTe thin films grown on STO. Figure 5 shows resistivity and Hall measurement results. As depicted in Fig. 5(a), FeTe thin film has a Neel temperature of 53 K which differs from that of single crystal, 68 K [15]. Another distinguishable feature of the resistivity of thin film in comparison to that of single crystal is the kink at 7 K (see the inset of Fig. 5(a)). Whereas there has been a report of superconductivity at 13K in FeTe under tensile strain which is a non-superconducting parent compound [17], 7 K kink we observe implies possible superconductivity due to tensile strain at the interface.

Furthermore, Hall measurements from 20 K to 70 K describe the carrier type change along with antiferromagnetic transition at 53 K (see Fig. 5(b)).

4. CONCLUSION

To sum up, we have successfully grown high-quality FeTe thin films on SrTiO₃ substrates which give 2% tensile strain to the system. Characterizations using RHEED, X-ray diffraction and AFM measurements show that our FeTe thin film samples are single-crystalline with flat surface. XPS results ensure that the samples are close to nominal stoichiometry. ARPES were used to explore the electronic structure. By means of transport properties, we report a sign of superconductivity in FeTe under tensile strain. These results can serve as a platform to study the magnetic and electronic phase space of iron chalcogenides which can be engineered as a function of Fe-Ch bond angle.

ACKNOWLEDGMENT

This work is supported by the Global Research Development Center (GRDC) Cooperative Hub Program through the National Research Foundation of Korea (NRF) funded by the Ministry of Science and ICT (MSIT) (Grant No. RS-2023-00258359) and the NRF grant funded by the Korean government (MSIT) (Grant No. NRF-2022R1A3B1077234).

REFERENCES

- [1] W. Li, et al., "Charge ordering in stoichiometric FeTe: Scanning tunneling microscopy and spectroscopy," *Phys. Rev. B*, vol. 93, pp. 041101(R), 2016.
- [2] P. Zhang, et al., "Observation of topological superconductivity on the surface of an iron-based superconductor," *Science*, vol. 360, pp. 182-186, 2018.
- [3] T. Shibauchi, et al., "Exotic superconducting states in FeSe-based materials," *J. Phys. Soc. Jpn.*, vol. 89, pp. 102002, 2020.
- [4] K. Kuroki, et al., "Pnictogen height as a possible switch between high-Tc nodeless and low-Tc nodal pairings in the iron-based superconductors," *Phys. Rev. B*, vol. 79, pp. 224511, 2009.

- [5] F. Wang, et al., "The electron-pairing mechanism of iron-based superconductors," *Science*, vol. 332, pp. 200-204, 2011.
- [6] A. Chubukov, et al., "Pairing mechanism in Fe-based superconductors," *Annu. Rev. Condens. Matter Phys.*, vol. 3, pp. 57-92, 2012.
- [7] I. I. Mazin, et al., "Unconventional superconductivity with a sign reversal in the order parameter of $\text{LaFeAsO}_{1-x}\text{F}_x$," *Phys. Rev. Lett.*, vol. 101, pp. 057003, 2008.
- [8] P. Hirschfeld, et al., "Gap symmetry and structure of Fe-based superconductors," *Rep. Prog. Phys.*, vol. 74, pp. 124508, 2011.
- [9] M. Yi, et al., "Role of the orbital degree of freedom in iron-based superconductors," *npj Quantum Materials*, vol. 2, no. 1, pp. 57, 2017.
- [10] M. Yi, et al., "Observation of universal strong orbital-dependent correlation effects in iron chalcogenides," *Nature Communications*, vol. 6, pp. 7777, 2015.
- [11] J. P. Locquet, et al., "Doubling the critical temperature of $\text{La}_{1.9}\text{Sr}_{0.1}\text{CuO}_4$ using epitaxial strain," *Nature*, vol. 394, pp. 453, 1998.
- [12] P. C. Klipstein, et al., "Stoichiometry dependence of the transport properties of TiS_2 ," *J. Phys. C: Solid State Phys.*, vol. 14, pp. 4067, 1981.
- [13] J. P. Reifenberg, et al., "Thickness and stoichiometry dependence of the thermal conductivity of GeSbTe films," *Appl. Phys. Lett.*, vol. 91, pp. 111904, 2007.
- [14] N. Bendiab, et al., "Stoichiometry dependence of the Raman spectrum of alkali-doped single-wall carbon nanotubes," *Phys. Rev. B*, vol. 64, pp. 245424, 2001.
- [15] Y. S. Kim, et al., "Kondo interaction in FeTe and its potential role in the magnetic order," *Nature communications*, vol. 14, pp. 4145, 2023.
- [16] S. Tan, et al., "Interface-induced superconductivity and strain-dependent spin density waves in FeSe/SrTiO₃ thin film," *Nature Materials*, vol. 12, pp. 634-640, 2013.
- [17] Y. Han, et al., "Superconductivity in iron telluride thin films under tensile stress," *Phys. Rev. Lett.*, vol. 104, pp. 017003, 2010.